

Ultrananocrystalline and Nanocrystalline Diamond Thin Films for MEMS/NEMS Applications

Anirudha V. Sumant, Orlando Auciello,
Robert W. Carpick, Sudarsan Srinivasan,
and James E. Butler

Abstract

There has been a tireless quest by the designers of micro- and nanoelectromechanical systems (MEMS/NEMS) to find a suitable material alternative to conventional silicon. This is needed to develop robust, reliable, and long-endurance MEMS/NEMS with capabilities for working under demanding conditions, including harsh environments, high stresses, or with contacting and sliding surfaces. Diamond is one of the most promising candidates for this because of its superior physical, chemical, and tribomechanical properties. Ultrananocrystalline diamond (UNCD) and nanocrystalline diamond (NCD) thin films, the two most studied forms of diamond films in the last decade, have distinct growth processes and nanostructures but complementary properties. This article reviews the fundamental and applied science performed to understand key aspects of UNCD and NCD films, including the nucleation and growth, tribomechanical properties, electronic properties, and applied studies on integration with piezoelectric materials and CMOS technology. Several emerging diamond-based MEMS/NEMS applications, including high-frequency resonators, radio frequency MEMS and photonic switches, and the first commercial diamond MEMS product—monolithic diamond atomic force microscopy probes—are discussed.

Brief Review of UNCD and NCD Growth Processes and Properties

Micro- and nanoelectromechanical systems (MEMS/NEMS) are an extension of integrated circuit technology, which consists of electrical and mechanical subsystems integrated together to convert physical stimuli and events to electrical, mechanical, and optical signals and vice versa. Due to their size (a few microns to a few tens of nanometers), a large number of devices could be batch-fabricated on a single wafer with enhanced functionality. Batch fabrication consumes less power and therefore would produce these single wafer devices more economically. Micro- and nanotechnology have been identified as

extremely promising technologies primarily for this reason. However, as the size of the devices shrinks, there are additional issues that arise due to the increased surface-to-volume ratio. Thus, surface and interface properties become dominant at this micro/nanoscale, driving the need to find suitable candidate materials. Diamond satisfies most of the expectations of MEMS/NEMS designers due to its extraordinary physical, chemical, and electrical properties. However, a number of technological challenges still need to be addressed.

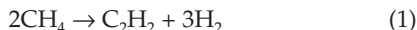
The pathway to the scale-up of diamond-based MEMS/NEMS requires the growth

of smooth diamond films with uniform thickness and micro/nanostructure over large area substrates (≥ 150 mm diameter wafer), as recently demonstrated.¹ Growth of thin (0.1 to 5 micron thick) diamond films on nondiamond substrates, typically conventional electronic substrates such as Si, SiC, and AlN, is performed as the initial step in the fabrication of diamond-based MEMS/NEMS. Diamond films are grown by chemical vapor deposition (CVD) using hot filament-activated or plasma-activated processes.²⁻⁴ Growth of diamond by CVD on nondiamond substrates requires a surface pretreatment, or "seeding," to enhance the nucleation of diamond grains, often by seeding/coating the substrate with small diamond nanoparticles.⁴ Conventional CVD film deposition methods employ microwave plasma-enhanced CVD or hot filament CVD with hydrogen-rich chemistry [H_2 (balance)/ CH_4 (0.1 to 4%)].²⁻⁴ Polycrystalline or microcrystalline diamond films, with thicknesses between 0.1–5 μm ,⁵ are produced when the initial nucleation density is low ($< 10^{10}/cm^2$). Microcrystalline diamond (MCD) films exhibit a columnar grain structure whose large grains (1–5 μm) coarsen with thickness. Correspondingly, they exhibit a rough, highly faceted morphology whose root mean square (RMS) roughness is typically $\sim 10\%$ of the film thickness. On the other hand, when very high nucleation densities are achieved ($> 10^{12}/cm^2$), relatively smooth, high-quality nanocrystalline diamond (NCD) films with thicknesses from 0.03–5 microns^{4,6} can be grown using 0.1 to 1% CH_4 in H_2 at temperatures of about 900°C. When the CH_4 content is increased to about 4%, smoother, fine-grained NCD films are grown, but with a higher percentage of nondiamond carbon (i.e., sp^2 bonds and noncrystalline configurations).

Once the diamond nuclei are present from the seeding process, growth is mostly homoepitaxial (including twinning and defect formation) on the seeds, with some nondiamond carbon incorporated in the grain boundaries. In this diamond CVD growth process, the principal carbon growth species are the CH_3 radicals.⁸⁻¹⁰ Atomic hydrogen is critical to drive the hydrogen abstraction reactions that (1) prepare the CH_3 adsorption site by removing a hydrogen atom from the hydrogen-terminated diamond surface and (2) abstract the hydrogen atoms from the adsorbed CH_3 and nearby surface sites, thereby permitting the carbon atom to insert into a diamond lattice site. The atomic hydrogen also preferentially etches the undesirable graphitic or amorphous carbon phases that might grow simultaneously with the diamond phase. Atomic hydrogen also etches

the diamond phase, but at a much lower rate. NCD films have a much smaller grain size (10–200 nm) and surface roughness (10–30 nm RMS) than microcrystalline diamond. The grain size and surface roughness of NCD films do not change substantially for a film thickness up to few microns due to the very high nucleation density, although the films still exhibit a columnar structure.⁶

After MCD and NCD, there is a third class of diamond thin films named ultrananocrystalline diamond (UNCD), which is grown using an Ar-rich/CH₄ chemistry in a microwave plasma-enhanced CVD process [Ar (99%)/CH₄ (1%)].^{4,11} (See Figure 1b–1c and Table I for a comparison of NCD and UNCD properties.) This chemistry produces carbon dimers (C₂) in the plasma, derived either from collision-induced fragmentation of methane in an Ar plasma or by thermal conversion via the following reactions:



While the Ar-rich/CH₄ plasma produces a complex mixture of carbon (C₂ dimers) and hydrocarbon species, including CH₃·, C₂H, C₂H₂, and other hydrocarbons, the C₂ dimers have been proposed to play a critical role in the UNCD nucleation and growth process.^{12,13} Calculations predict

that the C₂ dimers have a low activation energy (~6 kcal/mol) for insertion into the surface of the growing film, thus establishing the growth characteristic of UNCD.^{12,13} Recent modeling efforts have proposed that while the C₂ population in the plasma is high, the population near the surface is low, and other hydrocarbon radicals (e.g., CH₃·, C₂H) are also substantial participants in the growth.^{14,15} This model, however, could not fully explain the low temperature growth of UNCD with a modest growth rate. Clearly, more experimental studies are needed. Regardless of the mechanism, the distinctive characteristic of the UNCD film growth process is that the plasma contains very small quantities of hydrogen, which arise mainly from the thermal decomposition of methane to acetylene in the plasma (about 1.5%). Typical deposition conditions for the 2.45 GHz and 915 MHz microwave plasma-enhanced CVD reactors used in the growth of UNCD films are 1% CH₄/99% Ar. A unique outcome of the UNCD nucleation and growth processes is that these films are the only diamond films that have been demonstrated to grow at temperatures as low as 350–400°C on the wafer scale with complementary metal oxide semiconductor (CMOS) compatibility.¹ While the growth rate is modest (~0.1–0.2 μm/h),¹⁶ the low growth temperature opens the way for the development of

monolithically integrated UNCD-MEMS/NEMS/CMOS devices^{1,17} by integrating UNCD films with CMOS electronics, which have a very limited thermal budget. Currently, the variation in thickness uniformity of UNCD films on 150-mm and 200-mm diameter silicon wafers is approximately ±5% and ±11%, respectively; the 200-nm diameter is at the limit of today's microwave plasma technology, which accounts for the greater thickness variation.¹ The UNCD nucleation and growth process results in a nanostructure consisting of equiaxed 3–5 nm grains and atomically abrupt (~0.4 nm wide) grain boundaries for standard undoped UNCD,^{1,11} and approximately 7–10 nm grains and 1–2 nm grain boundaries for UNCD films grown with nitrogen in the gas mixture to achieve films with high electrical conductivity.¹⁸ Table I compares the measured properties of UNCD and NCD films. Figure 1a–1c shows scanning electron microscopy images of the surface morphology characteristics of MCD, NCD, and UNCD films, respectively, and Figure 1d–1e shows photographs of UNCD films deposited on 150-mm and 200-mm diameter silicon wafers using a 915 MHz microwave plasma-enhanced CVD system, respectively. Figure 1e is darker in the center due to thickness effects.

Mechanical and Nanotribological Studies of UNCD and NCD Thin Films

A strong argument for diamond-based MEMS/NEMS devices over those made from conventional silicon-based materials, particularly those involving sliding and rotational contacts, is the superior mechanical and tribological properties of UNCD and NCD. These properties depend not only on how the film is grown, but also on the nucleation pretreatment methods and the surface chemistry. The Young's modulus and hardness of UNCD^{19,20} and NCD⁶ have been shown to approach the values of single-crystal diamond, which is several times larger than for Si or SiO₂. The Poisson's ratio of hot filament CVD-grown UNCD has been recently reported to be 0.057±0.038,²⁰ and that for microwave plasma-grown NCD is 0.12±0.04,⁶ both of which are within the range of single-crystal diamond. Espinosa et al. have shown a strong dependence of the fracture strength²¹ of freestanding UNCD films on the nucleation pretreatment used. In one study, two seeding methods were compared, one involving the mechanical polishing of the silicon substrate using micron-size diamond powder and another using ultrasonic agitation of the silicon substrate in an alcohol solution containing

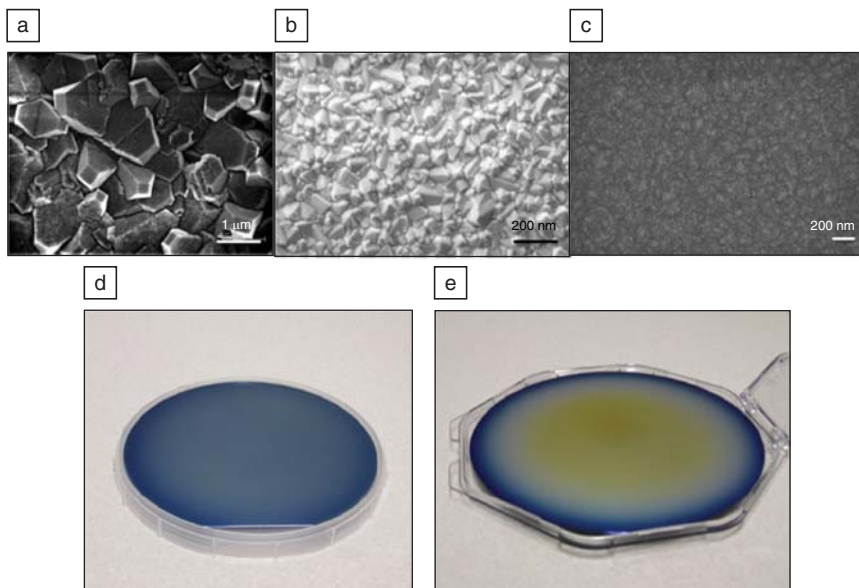


Figure 1. Scanning electron microscopy images showing typical surface morphology of (a) microcrystalline, reprinted with permission from Reference 60. ©2007, American Chemical Society; (b) nanocrystalline, and (c) ultrananocrystalline diamond (UNCD) films, reprinted with permission from Reference 24. ©2007, American Physical Society. Photographs of (d) a 150-mm-diameter Si wafer coated with a UNCD layer with ~5% variation in thickness uniformity, and (e) a 200-mm-diameter Si wafer coated with UNCD thin-film grown at 400°C. Reprinted with permission from Reference 1. ©2009, SPIE.

Table I. Comparison of the Properties of Highest Quality Ultrananocrystalline Diamond and Nanocrystalline Diamond Films.

Property	Ultrananocrystalline Diamond (UNCD)	Nanocrystalline Diamond (NCD)
Bonding Character	2–5% sp^2	<1% sp^2
Density (kg/m ³)	3,300	3,510
Young's Modulus (GPa)	980	1120
Hardness (GPa)	98	n.m.
Macroscopic Friction Coefficient	0.02–0.05	0.02–0.05
Macroscopic Wear Rate (mm ³ N ⁻¹ m ⁻¹)	1.8×10^{-8}	n.m.
Adhesion Energy (mJ/m ²) (measured using atomic force microscopy with diamond tip against UNCD surface)	10	n.m.
Surface Roughness (nm)	5–7	5–25
Fracture Toughness (MPa m ^{1/2})	4.7–7.2	n.m.
Grain Size (nm)	2–5	5–100
Sound Velocity (m/sec)	15,700	17,980
Thermal Conductivity (W/mK)	12	1370
Film Stress (MPa)	100	–100 to 300 Controllable
Deposition Temperature (°C)	400–800	450–950
UV-Vis Transmission	Semi-opaque	Transparent
Electrical Properties Conductivity/Resistivity/Mobility		
Undoped	n.m.	>10 ¹³ Ohm/sq. tan δ ~0.002
Nitrogen Incorporated	140–260 Ω^{-1} cm ⁻¹ Mobilities of 5–10 cm ² /Vsec	200 Ω^{-1} cm ⁻¹
Doped with Boron 10 ¹⁷ cm ⁻³	Mobilities of 90 cm ² /Vsec	Mobilities of 10–90 cm ² /Vsec
Doped with Boron >10 ²¹ cm ⁻³	10 Ω^{-1} cm ⁻¹	Superconducting at $T < 1.6$ K

Entries that have not been measured are abbreviated n.m. Reprinted with permission from Reference 4. ©2008, Wiley Interscience.

nanodiamond powder.²¹ In both cases, the behavior followed Weibull statistics, which indicates that preexisting flaws govern the brittle failure of the films. For nucleation by mechanical polishing, the fracture strength ranged from 1.74–2.26 GPa, whereas with ultrasonic seeding for nucleation, the fracture strengths increased to a range of 4.08–5.03 GPa. The range of values originates from a variation in the size of the largest defect in a given volume of material. With ultrasonic seeding, a much denser and smoother UNCD coating is achieved, minimizing the possibility of defect-prone regions at the underside of the film. Interestingly, subsequent experiments using Weibull statistics showed that the fracture strength scaled with the specimen volume, not the surface area.²¹ This indicates that the flaws occurring at the film-substrate interface are manifested in defective structure throughout the bulk of the film, and this highlights the critical roles that proper seeding and nucleation play.

Similar behavior is observed in the case of NCD films, where the effect of seeding density on the Young's modulus and thermal diffusivity were studied.⁶ The Young's moduli of the NCD films grown with lower nucleation densities (10¹⁰ cm⁻²) was roughly half of those of a film grown with much higher nucleation density ($\geq 10^{12}$ cm⁻²). For diamond grown with a high nucleation density, the Young's modulus was close to the corresponding values measured for single-crystal diamond or high-quality polycrystalline diamond films grown by CVD (1120 GPa). A higher nucleation density during growth leads to more rapid film coalescence and thus lower volumes of voids or nondiamond bonded carbon at the nucleation side (film/substrate interface). This, in turn, impacts the Young's modulus and fracture toughness of the films and also gives rise to a remarkably high thermal diffusivity.⁶

The surface chemistry, including the precipitation of amorphous carbon at the nucleation side as a function of different

types of nucleation treatment during the growth of NCD and UNCD films, was further investigated^{22–24} using surface-sensitive spectroscopies, including photoelectron emission microscopy coupled with near edge x-ray absorption fine structure spectroscopy (PEEM-NEXAFS), Auger electron spectroscopy, and x-ray photoelectron spectroscopy. These experiments enabled characterization of the chemistry and bonding configuration of UNCD and NCD surfaces and how this subsequently affects adhesion and friction. Since the underside of such films may be part of the tribological interface for given MEMS/NEMS geometries, this knowledge is important for the design and fabrication of reliable, working diamond-based MEMS/NEMS devices involving tribological contacts. For UNCD, nanotribological properties such as nanoscale adhesion (stiction) and friction on the nucleation side of the film were probed using atomic force microscopy (AFM) with a diamond AFM tip that mimics a single asperity contact of diamond against diamond (see Figure 2a–2b). The UNCD surface was subjected to hydrogen plasma treatment, which etches nondiamond carbon at the interface and leaves the UNCD surface H-terminated. Upon H-termination, the work of adhesion was reduced to only 10 mJ/m² from 59.2 mJ/m² measured before H-termination (Figure 2a). These low values approach the van der Waals' limit for attractive forces. In contrast, Si-Si contacts exhibited a work of adhesion of 826±186 mJ/m², which arises from hydrophilic interactions between the native oxide surfaces.²⁴ Nanoscale friction also was found to be reduced by more than a factor of two after H-termination (Figure 2b). From a tribological point of view, H-terminated UNCD surfaces performed similarly to H-terminated single-crystal diamond and much better than silicon.

Recent larger-scale friction measurements for self-mated UNCD interfaces have revealed low friction and wear²⁵ even under conditions considered unfavorable for diamond tribology, namely low relative humidities. Even at 1.0% relative humidity, friction coefficients of 0.04 were observed. Surface chemical imaging using PEEM-NEXAFS demonstrated that low friction was facilitated by the dissociative adsorption of water to form oxide-containing groups on the surface as well as some amorphous carbon with a higher percentage of sp^2 -hybridized bonds than as-grown UNCD. However, no evidence of crystalline graphite was detected, refuting the idea that has previously been proposed to explain the low friction of diamond surfaces. Studies of silicon nitride-UNCD

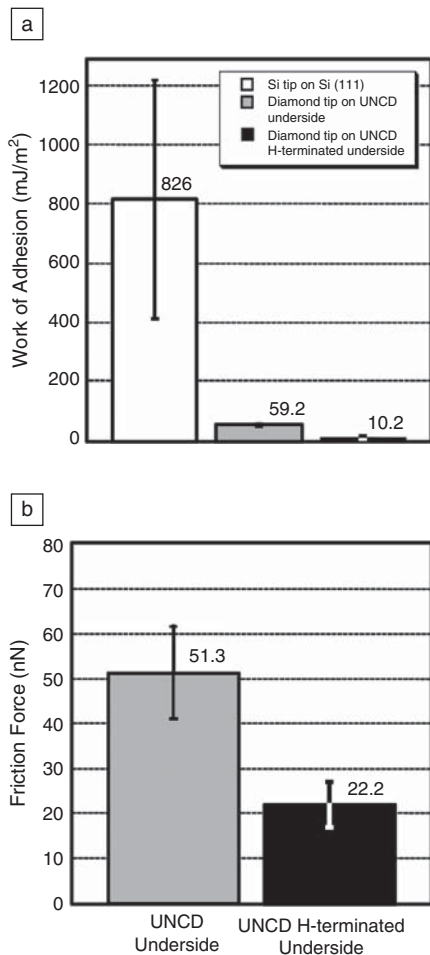


Figure 2. (a) Work of adhesion between a diamond-coated tip and ultrananocrystalline diamond (UNCD) nucleation side surfaces before and after H-termination. Results for a silicon tip making contact with a single-crystal silicon (111) wafer (both the tip and sample have a native oxide) are included for comparison. (b) Nanoscale friction force experienced by a diamond-coated tip scanning against the UNCD nucleation side surface before and after H-termination. Reprinted with permission from Reference 24. ©2007, American Physical Society.

interfaces also have revealed low friction even under high load conditions.^{26–28} These experiments demonstrate the possibility of controlling the nanoscale adhesion and friction properties of diamond by tuning the surface chemistry and the potential for diamond MEMS/NEMS to outperform conventional silicon.

Micromachining of UNCD and NCD Films for Fabrication of MEMS/NEMS Devices

Surface micromachining processes for fabricating UNCD- and NCD-based

MEMS/NEMS devices are mature and generally involve several steps, namely: (1) Seeding and subsequent growth of the UNCD/NCD film to the desired thickness on a silicon wafer coated with a sacrificial thermal oxide layer (of appropriate thickness), (2) deposition of a blanket layer, as the etch mask, on the surface of diamond film followed by lithography and patterning, (3) reactive ion etching (RIE) of the undesired diamond unprotected by the mask, and (4) either dry (RIE) or wet (acid etch) chemistry to dissolve the sacrificial SiO₂ to release the final structure.^{30–33} Materials used for etch masks to protect the diamond during RIE include metals (Cr, Al, Ni), sputtered SiO₂, and some special photoresists. One such photoresist is HSQ Fox-17. The HSQ is spin-coated and subsequently baked at elevated temperatures (100–400°C) for a few minutes to form a very thin (50–80 nm) oxide layer on top of the diamond. The HSQ acts as a negative photoresist suitable for e-beam lithography. It has been recently demonstrated that the combination of HSQ photoresist and e-beam lithography can be used to fabricate UNCD nanowires ~20 nm wide and nanostructures of different shapes with dimensions down to 10 nm, dimensions that have not been achieved before. The fabrication of NEMS structures using UNCD layers requires the use of an appropriate seeding^{34,35} method to form dense, continuous diamond films with thicknesses in the 30–80 nm range. Similarly, NEMS structures with line widths down to 30 nm have been demonstrated in NCD films using e-beam lithography.²⁹

Electrically conducting boron-doped NCD films can be incorporated in more complex MEMS structures, resulting in GHz resonators with high-quality factors (Qs) exceeding 10,000 in ambient air and reasonably low electrical insertion loss.³⁶ Photonic nano- and microstructures have similarly been fabricated in NCD^{37,38} films and single-crystal diamond films.^{39–41}

Integration of UNCD with Piezoelectric Materials and CMOS

Low-voltage MEMS/NEMS actuation, in general, can be achieved using piezoelectric actuation. In such a case, a piezoelectric layer sandwiched between two electrode layers deposited on the structural MEMS/NEMS component is deformed mechanically upon application of a low voltage between the electrode layers, resulting in motion of the MEMS/NEMS structure (e.g., cantilever). In this respect, piezoelectric Pb(Zr_xTi_{1-x})O₃ (PZT) films, with excellent piezoelectric

and electromechanical coupling coefficients and high remnant polarization, are being investigated for application to Si-based MEMS devices.^{42,43} The high-force generated from a piezo-layer upon application of voltage between the top and bottom electrodes sandwiching that layer yields efficient micro/nanoactuators.⁴³ The piezoelectric coupling coefficients of PZT films are much higher ($d_{31} = -59$ pC/N, $e_{31,f} = -8$ to -12 C/m² for epitaxial films) than those of other piezoelectric materials, such as ZnO ($e_{31,f} = -1$ C/m²) and AlN ($d_{31,f} = -1.98$ pC/N, $e_{31,f} = -1.05$ C/m², where $e_{31,f}$ is the effective piezoelectric constant). Piezoelectric actuation using PZT films can be achieved with low voltages (≤ 5 V), depending on the film thickness. Since PZT has a relatively low Young's modulus (80 GPa), which is even lower than that of Si (130 GPa), it would not be an appropriate material as a structural component for MEMS/NEMS devices, such as resonators, which would require a structural material with a high Young's modulus. Therefore, PZT should be integrated with an appropriate structural material. Researchers are investigating the integration of PZT with Si for piezo-actuated Si-based MEMS/NEMS devices.^{42,43} However, the Young's modulus of Si is still relatively low. UNCD and NCD, with moduli essentially that of single-crystal diamond (980 to 1220 GPa),⁴ provide a much better platform of structural material for integration with piezoelectric layers. In this respect, it has been recently demonstrated⁴⁴ that UNCD-based MEMS/NEMS can be actuated using the piezoelectric phenomena, via integration of PZT layers with UNCD cantilevers. This achievement required new materials integration strategies to integrate an oxide piezoelectric layer such as PZT, generally grown by sputter-deposition or metal-organic CVD in an oxygen environment at a relatively high temperature (~500–700°C). Previously, these growth processes would have resulted in chemical etching of the carbon-based UNCD layer, via formation of volatile CO and CO₂ molecules.

The integration of PZT and UNCD films can be achieved by using robust TiAl or TaAl (named TA) layers with dual functionality as oxygen diffusion barriers and adhesion layers interposed between PZT and UNCD layers. Fan et al.⁴⁵ proposed the TA barriers on thermodynamic arguments, which indicate that oxygen atoms react preferentially with Ti, Ta, and Al to form stable oxides due to the lowest energy of oxide formation for these elements with respect to all other elements in the periodic

table. The oxygen barrier functionality of TiAl layers was first demonstrated in work focused on integration of $\text{BaSr}_x\text{Ti}_{1-x}\text{O}_3$ films with Cu electrode layers to produce high-performance Cu/BST/Cu capacitors for high-frequency devices.⁴⁵ The first hybrid piezoelectrically actuated PZT/UNCD MEMS cantilevers and NEMS horizontal switches were recently demonstrated,^{44,46} which were actuated with 3 V and 1 V respectively (Figure 3a–3b).

UNCD Integration with CMOS

In addition to the integration of UNCD with other technologically significant materials, it is important to develop a synthesis process that would enable the integration of UNCD films with CMOS devices. This, in turn, will provide the basis for the production of a new generation of monolithically integrated diamond MEMS/NEMS/CMOS devices for low-power CMOS-driven MEMS/NEMS-based systems. In this respect, it has been demonstrated that the UNCD films can be synthesized at $\leq 400^\circ\text{C}$,¹⁶ within the temperature limit that CMOS devices can withstand. The compatibility of the low-temperature UNCD process with CMOS was tested by depositing UNCD films directly on the CMOS wafer and testing the performance of CMOS devices before and after the UNCD deposition.¹ Figure 4a shows the schematics for the integration of UNCD films with CMOS chips, while Figure 4b shows the corresponding cross-section scanning electron microscopy (SEM) image of the integrated UNCD/CMOS structure. Electrical measurements of CMOS devices before and after UNCD deposition (Figure 4c–4d) demonstrated that all devices perform to specifications before and after UNCD deposition. This is a significant achievement that opens the pathway for the development of a new generation of monolithically integrated diamond-MEMS/NEMS/CMOS devices.

MEMS/NEMS Applications of UNCD and NCD Resonators

Following the success of MEMS mechanical resonators based on Si, the diamond materials discussed previously were explored as early as 1990 for mechanical structures due to the expected higher stiffness,⁴⁷ and the field grew significantly as NCD⁶ and UNCD¹⁷ matured. In 2002, the initial diamond NEMS structures exhibited the highest (then) attainable frequencies²⁹ and eventually achieved GHz frequencies with a disk resonator geometry (Figure 5) in 2004,³⁶ with quality factors exceeding 10,000 even in air. (The quality factor is a

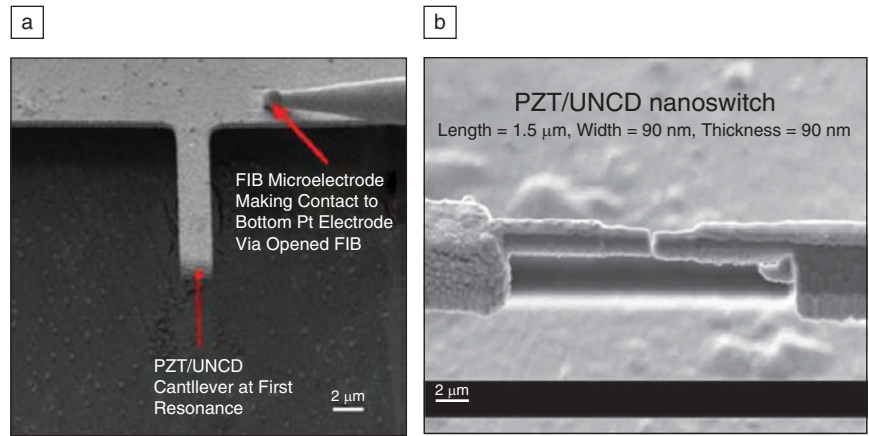


Figure 3. (a) Scanning electron microscopy (SEM) of hybrid PZT/ultranananocrystalline diamond (UNCD) microresonator vibrating at its resonance frequency and (b) a SEM of PZT/UNCD nanoelectromechanical systems switch (fabricated using focused ion beam [FIB]) driven with 1 V at 1 MHz oscillating for one billion cycles. (a) Reprinted with permission from Reference 44. ©2007, American Institute of Physics.

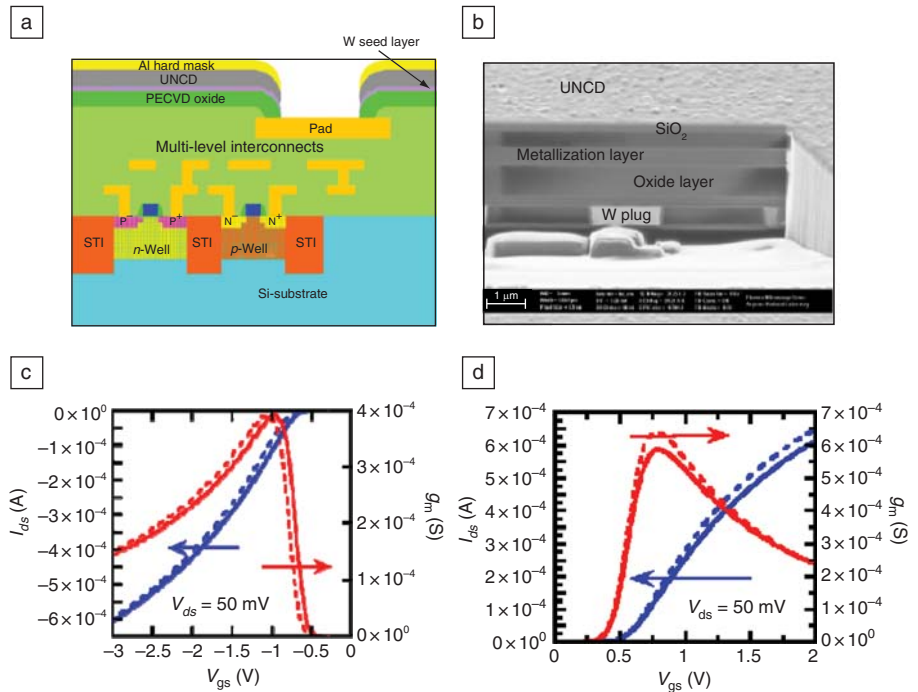


Figure 4. (a) Cross-section schematics of a complementary metal oxide semiconductor (CMOS) chip showing an ultrananocrystalline diamond (UNCD) deposition scheme and (b) a corresponding focused ion beam cross-section scanning electron microscopy image of the UNCD-deposited CMOS chip. (c–d) Electrical performance of the PMOS and NMOS devices before (solid lines) and after (dashed lines) UNCD deposition at 400°C . (b) Reprinted with permission from Reference 1. ©2009, SPIE. g_m , transconductance; I_{ds} , current between drain and source; PECVD, plasma-enhanced chemical vapor deposited; V_{ds} , voltage between drain and source.

dimensionless parameter that characterizes an oscillator's bandwidth and is an indirect measure of mechanical dissipation.) In 2006, NCD-based phononic structures (coupled mechanical resonator arrays) were produced.³⁷ UNCD-based resonators,

simple cantilever beams fixed at both ends, also were fabricated. Preliminary measurements of the linear UNCD resonators performance showed that UNCD exhibits the highest acoustic velocity ($\sim 15,000$ m/s) to date for a diamond film

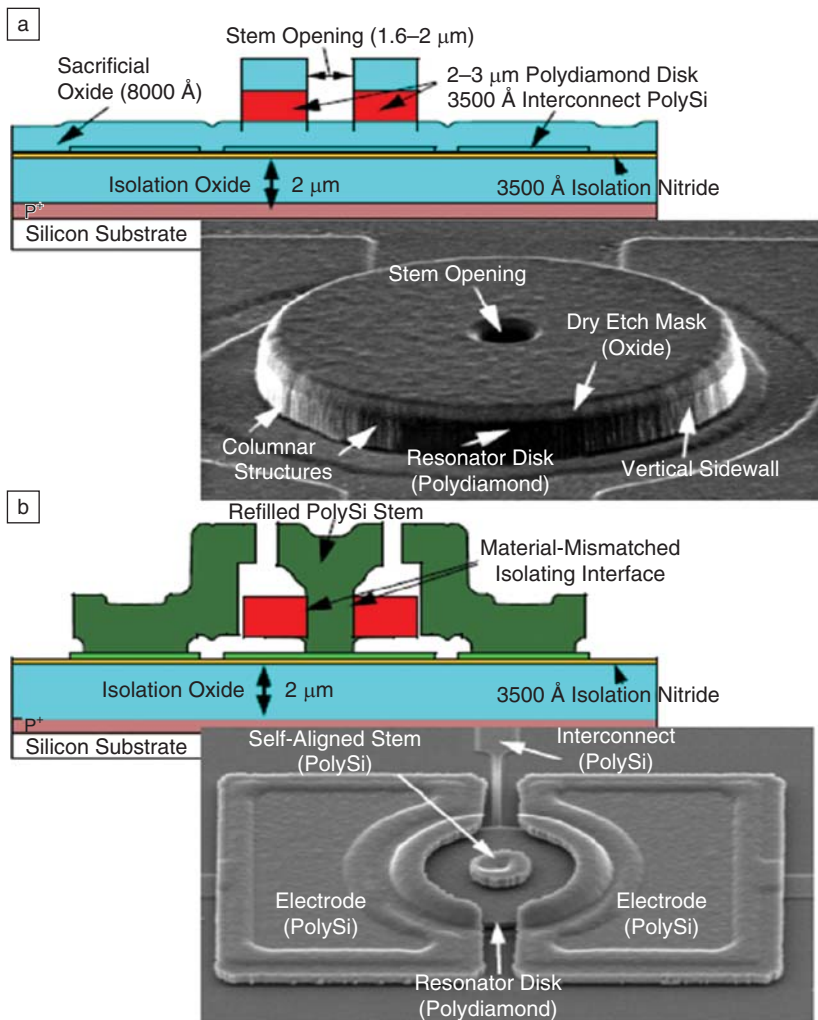


Figure 5. Cross-sectional schematic of the fabrication process and associated scanning electron microscopy pictures at different stages of the process related to fabrication of diamond disk resonator, which operates at 1.51 GHz with a Q of 11,555. (a) After diamond disk definition (disk diameter is 20 μm) and (b) after polysilicon stem refilling and electrode definition (width of rectangle is 60 μm). Reprinted with permission from Reference 31. ©2002, IEEE.

deposited at temperatures as low as 550°C.¹³ Cantilever-type microresonators fabricated in UNCD demonstrated quality factors as high as 16,000 in vacuum at ~kHz resonance frequencies.²⁰ A primary driver for the development of these high-frequency mechanical resonators was the development of communication filters and radio frequency signal processing devices. In addition, it was realized that these mechanical resonators would also be excellent mass and chemical sensors,^{48,49} particularly if the chemical termination⁵⁰⁻⁵² of the surface could be controlled. It was soon discovered that sensitivity and better response time of the resonators can be obtained by going to higher frequencies and therefore reducing device dimensions down to the nanoscale. However, at the nanoscale, due to the increase in surface-

to-volume ratio, surface dissipation mechanisms can limit the quality factors. However, surface stability and high stiffness of the UNCD means that high-frequency resonators with high-quality factors are feasible.²⁰ In the case of NCD and UNCD²⁰ films, which have a large fraction of grain boundaries, it has been demonstrated that defects at the grain boundaries are mainly responsible for the mechanical dissipation, triggering the need for fundamental studies relating the atomic structure to various dissipative mechanisms in these materials.

Additionally, it has been shown that these grain boundaries in NCD and UNCD can be doped with hydrogen, making them excellent leaky dielectric materials, and their use in radio frequency-MEMS capacitive switches as an insulating dielectric has

been demonstrated.^{53,54} In case of UNCD, the charging and discharging time constants are measured to be 100 μs , five to six orders of magnitude faster than those of conventional insulating dielectric films, and 12 billion cycles of operations have been demonstrated.⁵⁴ These results demonstrate a new paradigm in MEMS switch operation, and for the first time, this offers the possibility of operating capacitive MEMS switches almost continuously “on” without an adverse effect on switch reliability.

Optical resonator structures³⁸ and photonic crystals^{39,43} are also possible with NCD NEMS fabrication and eventually may be integrated with mechanical resonator structures for optical transduction of the mechanical motion. Figure 6a–6c shows SEM images of a fabricated photonic crystal resonator structure³⁸ based on NCD, and Figure 6d shows a SEM picture of coupled ring resonators, a precursor to phononic crystal structures, and the corresponding model analysis of the different mechanical modes.

Fabrication of Monolithic UNCD AFM Tips and Related Applications

The technology for fabricating monolithic UNCD AFM cantilevers with integrated tips has been recently developed,^{55,57} and UNCD AFM probes, including ones that are electrically conducting (boron doped), are now commercially available (Figure 7a).⁵⁶ Monolithic diamond AFM tips take advantage of diamond’s high Young’s modulus, allowing high-frequency tapping mode operation of the AFM and higher sensitivity, which could not be achieved using previous diamond-coated Si tips. They represent the first MEMS-type structures in the market based on UNCD. Tests have demonstrated that UNCD AFM tips can exhibit practically no wear after extensive scanning on different surfaces as opposed to the high wear generally observed with conventional Si and Si_3N_4 -based AFM tips. Figure 7b shows the comparison of tip volume loss versus distance scanned for UNCD and silicon nitride AFM tips during wear testing. The tips were worn by scanning them against a UNCD surface using a defined wear protocol, and the tip shape was periodically measured with electron microscopy and an AFM tip reconstruction method. Tips were tested at two humidity levels, as indicated, and all had similar initial shapes and radii. The UNCD tips exhibit little wear. However, the commercial silicon nitride tips wear significantly, with the volume loss substantially increased at elevated humidity levels due to tribochemical wear of silicon nitride.⁵⁷

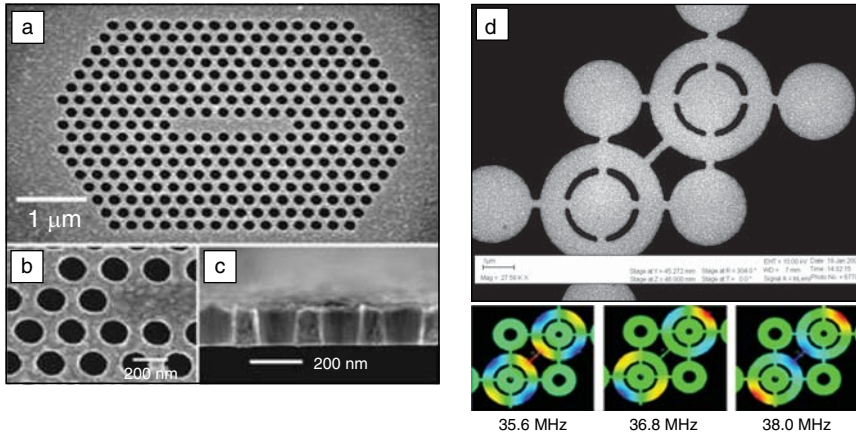


Figure 6. (a) Scanning electron microscopy (SEM) image of a suspended photonic crystal membrane cavity with holes (photonic crystal lattice parameter, $a = 240$ nm and hole radius, $r = 80$ nm); (b) high magnification picture of holes; (c) cross-sectional image of holes. The membrane is ~ 160 nm thick, while the sidewall of the holes is tilted by 3° . Reprinted from with permission from Reference 38. ©2007, American Institute of Physics. (d) SEM (top) picture and (bottom) model analysis of first three modes of nanocrystalline diamond ring resonators coupled as part of a phononic crystal resonator array with increased coupling via flexural beams. Reprinted with permission from Reference 48. ©2006, Elsevier.

These probes will find applications in metrology, AFM imaging in corrosive liquids, and nanoscale electrical measurements of nanostructures. One of the possible applications could be in a high-density data storage system consisting of ferroelectric layers, where data could be stored via electric field-induced polarization upon application of a voltage pulse, or phase change films, via change of resistivity upon application of voltage pulses.⁵⁸ In both cases, good tribomechanical properties using UNCD would be useful during interaction of the tip with the memory element to imprint the information.

Ultra-Smooth Diamond Films:

Although the as-grown roughness of UNCD (Figure 7a) and NCD films are very low (~ 5 – 7 nm), achieving roughness ≤ 1 nm RMS for UNCD surfaces would further expand the applications of UNCD films, particularly for NEMS devices where atomic-scale roughness may be critical. UNCD thin films on 150-mm diameter silicon wafers with surface roughness ≤ 1 nm are now commercially available (Figure 7b).⁵⁹ The extremely smooth UNCD films are produced using a chemical mechanical planarization process. These smooth diamond films will allow growth of highly oriented PZT and AlN thin film on diamond, leading to better electromechanical coupling, and may enable fabrication of higher performance resonators and surface acoustic wave devices. Other potential applications areas include nanophotonics, biosensors, biomedical, and nanoimprint lithography.

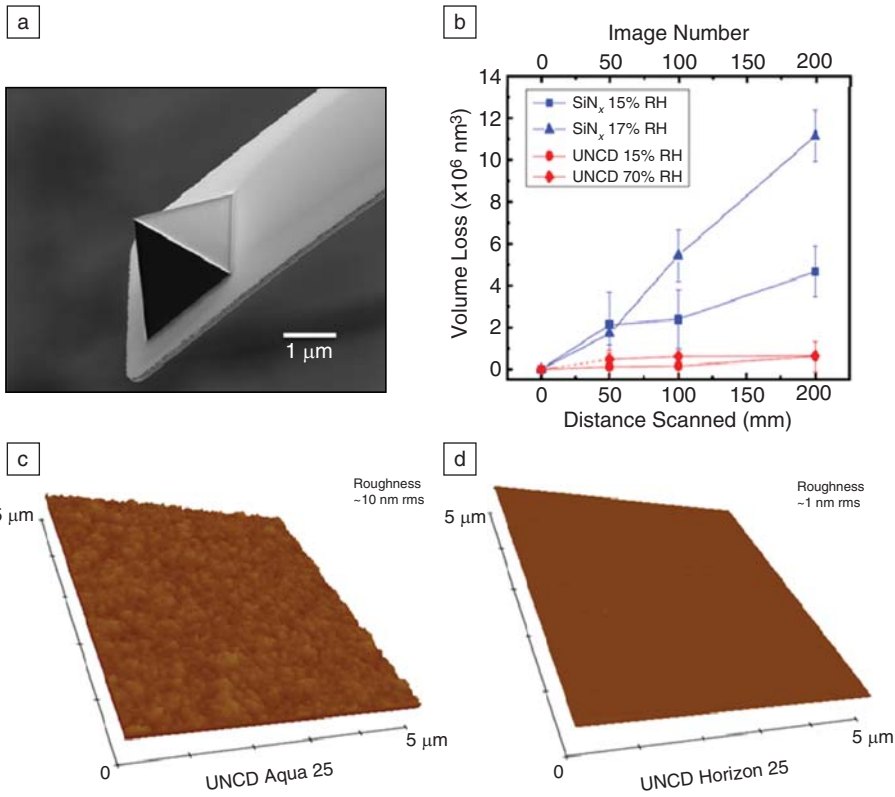


Figure 7. (a) Scanning electron microscopy image of commercially available microfabricated monolithic ultrananocrystalline diamond (UNCD) atomic force microscopy (AFM) tip (image courtesy of Advanced Diamond Technologies, Inc.) and (b) a comparison of wear performance with that of a Si₃N₄ tip. Reprinted with permission from Reference 57. ©2010, Wiley Interscience. (c) AFM images of as-grown UNCD film (Aqua 25) and (d) after chemical mechanical planarization polishing (Horizon 25) showing extremely smooth surface morphology (root mean square roughness: ~ 1 nm). AFM scanning areas in both images are $5 \mu\text{m} \times 5 \mu\text{m}$. Images courtesy of Advanced Diamond Technologies, Inc.

Conclusions

The current status of diamond thin-film technology for applications in fabricating micro- and nanoelectro-mechanical system (MEMS/NEMS) devices is reviewed. Although silicon has been the material of choice for the development of MEMS/NEMS devices, average mechanical and tribological properties of silicon are detrimental to developing robust, reliable MEMS/NEMS devices involving sliding and rotating contacts or operating in harsh conditions. Ultrananocrystalline diamond and nanocrystalline diamond thin-film technologies are mature enough to enable a new generation of multifunctional MEMS/NEMS devices with a long life and a performance that is orders of magnitude better than Si-based MEMS and NEMS. This is evident from the first diamond-based MEMS product, a monolithic atomic force microscopy tip that has demonstrated much-improved performance compared to its silicon and silicon nitride counterparts.

Likewise, several new technologies based on diamond, such as high-frequency resonators and radio frequency-MEMS, are promising, and consistent efforts on fundamental studies and applications will provide the basis for the insertion of diamond MEMS/NEMS in the market.

Acknowledgments

A.V.S. and O.A. acknowledge the use of the Center for Nanoscale Materials supported by the U.S. Department of Energy, Office of Science, Office of Basic Energy Sciences, under Contract No. DE-AC02-06CH11357, and DARPA under contract MIPR 06-W238. They also acknowledge the contributions of several colleagues, including J.A. Carlisle, J. Hiller, B. Kabius, D.C. Mancini, S. Pacheco, and Z. Ma. J.E.B. acknowledges the support of the Office of Naval Research/Naval Research Laboratory and DARPA. R.W.C. acknowledges support from Air Force Office of Scientific Research grant FA9550-08-1-0024. He also gratefully acknowledges the contributions of D.S. Grierson, A.R. Konicek, V.P. Adiga, W.G. Sawyer, and P.U.P.A. Gilbert. The authors acknowledge J.A. Carlisle and Neil Kane from Advanced Diamond Technologies Inc. for providing images of the NaDiaProbe and Horizon UNCD films.

References

1. A.V. Sumant, O. Auciello, H.-C. Yuan, Z. Ma, R.W. Carpick, D.C. Mancini, *Proc. SPIE* **7318**, 17 (2009).
2. J.E. Butler, H. Windischmann, *MRS Bull.* **23** (9), 22 (1998).
3. M.A. Prelas G. Popovici, K.L. Biglow, Eds. (Marcel Dekker, NY, 1997); R.S. Sussmann, Ed., *Handbook of Industrial Diamonds and Diamond Films* (Wiley, Chichester, UK, 2009).
4. J.E. Butler, A.V. Sumant, *Chem. Vap. Deposition* **14** (7–8), 145 (2008).
5. D. Das, R.N. Singh, *Int. Mater. Rev.* **52** (1), 29 (2007).
6. J. Philip, P. Hess, T. Feygelson, J.E. Butler, S. Chattopadhyay, K.H. Chen, L.C. Chen, *J. App. Phys.* **93** (4), 2164 (2003).
7. J.E. Butler, personal communication.
8. J.E. Butler, R.L. Woodin, *Philos. Trans. R. Soc. London, Ser. A* **342** (1664), 209 (1993).
9. J.E. Butler, A. Cheesman, M.N.R. Ashfold, in *CVD Diamond for Electronic Devices and Sensors*, R.S. Sussmann, Ed. (Wiley, Chichester, UK, 2009), pp. 103–124.
10. J.E. Butler, Y.A. Mankelevich, A. Cheesman, J. Ma, M.N.R. Ashfold, *J. Phys.: Condens. Matter* **21**, 364201 (2009).
11. S. Jiao, A.V. Sumant, M.A. Kirk, D.M. Gruen, A.R. Krauss, O. Auciello, *J. Appl. Phys.* **90**, 118 (2001).
12. D.M. Gruen, *MRS Bull.* **23** (9), 32 (1998).
13. M. Sternberg, P. Zapol, L.A. Curtiss, *Phys. Rev. B* **68**, 205330 (2003).
14. P.W. May, N.L. Allan, M.N.R. Ashfold, J.C. Richley, Y.A. Mankelevich, *J. Phys.: Condens. Matter* **21**, 364203 (2009).
15. P.W. May, J.N. Harvey, J.A. Smith, Y.A. Mankelevich, *J. Appl. Phys.* **99** (2006).
16. X. Xiao, J. Birrell, J. Gerbi, O. Auciello, J.A. Carlisle, *J. Appl. Phys.* **96**, 2232 (2004).
17. O. Auciello, S. Pacheco, A.V. Sumant, C. Gudeman, S. Sampath, A. Datta, R.W. Carpick, V.P. Adiga, P. Zurcher, Z. Ma, H.C. Yuan, J.A. Carlisle, B. Kabius, J. Hiller, *IEEE Microwave Mag.* **8**, 61 (2008).
18. J. Birrell, J.A. Carlisle, O. Auciello, D.M. Gruen, J.M. Gibson, *Appl. Phys. Lett.* **81** (12), 2235 (2002).
19. H.D. Espinosa, B.C. Prorok, B. Peng, K.H. Kim, N. Moldovan, O. Auciello, J.A. Carlisle, D.M. Gruen, D.C. Mancini, *Exp. Mech.* **43**, 256 (2003).
20. V.P. Adiga, A.V. Sumant, S. Suresh, C. Gudeman, O. Auciello, J.A. Carlisle, R.W. Carpick, *Phys. Rev. B* **79**, 245403 (2009).
21. H.D. Espinosa, B. Peng, B.C. Prorok, N. Moldovan, O. Auciello, J.A. Carlisle, D.M. Gruen, D.C. Mancini, *J. Appl. Phys.* **94**, 6076 (2003).
22. A.V. Sumant, D.S. Grierson, J.E. Gerbi, J. Birrell, U.D. Lanke, O. Auciello, J.A. Carlisle, R.W. Carpick, *Adv. Mater.* **17**, 1039 (2005).
23. A.V. Sumant, P. Gilbert, D.S. Grierson, A.R. Konicek, M. Abrecht, J.E. Butler, T. Feygelson, S.S. Rotter, R.W. Carpick, *Diamond Relat. Mater.* **16** (4–7), 718 (2007).
24. A.V. Sumant, D.S. Grierson, J.E. Gerbi, J. Carlisle, O. Auciello, R.W. Carpick, *Phys. Rev. B* **76**, 235429 (2007).
25. A.R. Konicek, D.S. Grierson, P.U.P.A. Gilbert, W.G. Sawyer, A.V. Sumant, R.W. Carpick, *Phys. Rev. Lett.* **100**, 235502/1–4 (2008).
26. A. Erdemir, C. Bindal, G.R. Fenske, C. Zuiker, A.R. Krauss, D.M. Gruen, *Diamond Relat. Mater.* **5**, 923 (1996).
27. A. Erdemir, G.R. Fenske, A.R. Krauss, D.M. Gruen, T. McCauley, R.T. Csencsits, *Surf. Coat. Technol.* **565**, 120 (1999).
28. D.S. Grierson, A.V. Sumant, A.R. Konicek, M. Abrecht, J. Birrell, O. Auciello, J.A. Carlisle, T.W. Scharf, M.T. Dugger, P.U.P.A. Gilbert, R.W. Carpick, *J. Vac. Sci. Technol., B* **25**, 1700 (2007).
29. L. Sekaric, J.M. Parpia, H.G. Craighead, T. Feygelson, B.H. Houston, J.E. Butler, *Appl. Phys. Lett.* **81** (23), 4455 (2002).
30. J.W. Baldwin, M. Zalalutdinov, T. Feygelson, J.E. Butler, B.H. Houston, *J. Vac. Sci. Technol., B* **24** (1), 50 (2006).
31. W. Jing, J.E. Butler, D.S.Y. Hsu, C.T. Nguyen, *Micro Electro Mechanical Systems*, 2002, The 15th IEEE International Conference (2002), pp. 657–660.
32. J. Kusterer, E. Kohn, *CVD Diamond for Electronic Devices and Sensors*, R.S. Sussmann, Ed. (Wiley, Chichester, UK, 2009), pp. 469–545.
33. A.R. Krauss, O. Auciello, D.M. Gruen, A. Jayatissa, A.V. Sumant, J. Tucek, D.C. Mancini, N. Moldovan, A. Erdemir, D. Ersoy, M.N. Gardos, H.G. Busmann, E.M. Meyer, M.Q. Ding, *Diamond Relat. Mater.* **10**, 1952 (2001).
34. S. Rotter, *Diamond Films Technol.* **6** (6), 331 (1996).
35. N.N. Naguib, J.W. Elam, J. Birrell, J. Wang, D.S. Grierson, B. Kabius, J.M. Hiller, A.V. Sumant, R.W. Carpick, O. Auciello, J.A. Carlisle, *Chem. Phys. Lett.* **430**, 345 (2006).
36. W. Jing, J.E. Butler, T. Feygelson, C.T. Nguyen, *Micro Electro Mechanical Systems 17th IEEE International Conference on MEMS*, **641** (2004).
37. C.F. Wang, Y.S. Choi, J.C. Lee, E.L. Hu, J. Yang, J.E. Butler, *Appl. Phys. Lett.* **90** (8) (2007).
38. C.F. Wang, R. Hanson, D.D. Awschalom, E.L. Hu, T. Feygelson, J. Yang, J.E. Butler, *Appl. Phys. Lett.* **91**, 20112 (2007).
39. M.P. Hiscocks, C.J. Kaalund, F. Ladouceur, B.C. Gibson, S. Trpkovski, S.T. Huntington, D. Simpson, E. Ampem-Lassen, F. Hossain, L. Hollenberg, S. Prawer, J.E. Butler, *Processing of Diamond: Towards All-Diamond Integrated Optics*. COIN-ACOFT 2007—International Conference on Optical Internet held jointly with the 32nd Australian Conference on Optical Fiber Technology (2007), pp. 296–298.
40. C.F. Wang, E.L. Hu, J. Yang, J.E. Butler, *J. Vac. Sci. Technol. B* **25** (3), 730 (2007).
41. M.P. Hiscocks, K. Ganesan, B.C. Gibson, S.T. Huntington, F. Ladouceur, S. Prawer, *Optics Express* **16** (24), 19512 (2008).
42. D. Polla, *MRS Bull.* **21**(6) (1996).
43. P. Muralt, *Int. J. Comput. Eng. Sci.* **4**(2), 163 (2003).
44. S. Sudarsan, J. Hiller, B. Kabius, O. Auciello, *Appl. Phys. Lett.* **90**, 134101 (2007).
45. W. Fan, S. Saha, J.A. Carlisle, O. Auciello, R.P.H. Chang, R. Ramesh, *Appl. Phys. Lett.* **82** (9), 1452 (2003).
46. O. Auciello, S. Srinivasan, J. Hiller, A.V. Sumant, B. Kabius, *Proc. SPIE* **7318**, 18 (2009).
47. J.L. Davidson, R. Ramesh, C. Ellis, *J. Electrochem. Soc.* **137** (10), 3206 (1990).
48. J.W. Baldwin, M.K. Zalalutdinov, T. Feygelson, B.B. Pate, J.E. Butler, B.H. Houston, *Diamond Relat. Mater.* **15** (11–12), 2061 (2006).
49. K.L. Ekinici, M.L. Roukes, *Rev. Sci. Instrum.* **76** (6) (2005).
50. J.S. Hovis, S.K. Coulter, R.J. Hamers, M.P. D'Evelyn, J.N. Russell, J.E. Butler, *J. Am. Chem. Soc.* **122** (4), 732 (2000).
51. T. Strother, T. Knickerbocker, J.N. Russell, J.E. Butler, L.M. Smith, R.J. Hamers, *Langmuir* **18** (4), 968 (2002).
52. W.S. Yang, O. Auciello, J.E. Butler, W. Cai, J.A. Carlisle, J. Gerbi, D.M. Gruen, T. Knickerbocker, T.L. Lasseter, J.N. Russell, L.M. Smith, R.J. Hamers, *Nat. Mater.* **1** (4), 253 (2002).
53. S. Balachandran, D. Hoff, A. Kumar, T. Weller, *IEEE MTT-S Int. Microwave Symp. Dig.* 1657 (2009).
54. C. Goldsmith, A. Sumant, O. Auciello, J. Carlisle, H. Zeng, J.C.M. Hwang, C. Palego, et al. *IEEE Int. Microwave Symp. Dig.* in press (2010).
55. K.-H. Kim, N. Moldovan, C. Ke, H.D. Espinosa, X. Xiao, J.A. Carlisle, O. Auciello, *Small*, **1** (8–9), 866 (2005).
56. NadiaProbe brochure; www.thindiamond.com/NaDiaProbes.asp.
57. J. Liu, D.S. Grierson, N. Moldovan, J. Notbohm, S. Li, P. Jaroenapibal, S.D. O'Connor, et al. *Small*, in press (2010).
58. O. Auciello, U.S. patent 7,602, 105 (October 13, 2009).
59. UNCD Horizon brochure; www.thindiamond.com/Diamond_Wafers.asp.
60. G. Gao, R.J. Cannara, R.W. Carpick, J.A. Harrison, *Langmuir*, **23** (10), 5394 (2007). □

COMMERCIALY
AVAILABLE
◆ UNCD Wafers ◆



UNCD® Wafers are wafer-scale diamond products used for MEMS development, tribological testing and unique nano-scale processing applications. UNCD Wafers offer the ability to create and experiment with the extraordinary properties of diamond using the award winning family of UNCD materials. UNCD Wafers meet a set of baseline wafer-level specifications for thickness and property uniformity, wafer bow, and particle counts suitable for direct insertion into a MEMS foundry process sequence.



Thin.



Smooth.



Diamond.

Immediately Available:

DoSi - Diamond on Silicon
DOI - Diamond on Insulator

Wafer Sizes: 100mm 150mm 200mm 300mm

Custom MEMS development, wafer scale foundry processing, small lot sizes, diamond on patterned wafers, diamond on specialty wafers and additional wafer sizes are also available.

UNCD
A Family of Diamond Materials

	Chemically Inert	Thermally Conductive	Electrically Conductive	Smooth Surface		
				>10nm	~7nm	<1nm
Aqua 25	◆	◆				◆
Aqua 50	◆	◆◆				◆
Aqua 100	◆	◆◆◆				◆
Lightning 25	◆	◆	◆			
Horizon Lightning 25	◆	◆	◆			◆
Horizon Aqua 25	◆	◆				◆
UNCD Windows	◆	◆				

Devices made using UNCD Wafers include all-diamond AFM probes (NaDiaProbes), bio-sensing cantilevers and membranes, free-standing diamond membranes, nano-imprint lithography molds, heat transfer base layers in MEMS devices, 3-D diamond structures on a wafer scale, radio-frequency (RF) switches, RF resonators and water purification electrodes.



Best practices and etch recipes can be found at www.thindiamond.com or email us at sales@thindiamond.com

For pricing, availability and specifications, visit:

www.thindiamond.com

